NASA TECHNICAL NOTE

NASA TN D-7116

NASA TN D-7116

POSITION DETERMINATION ACCURACY FROM THE MICROWAVE LANDING SYSTEM

by Luigi S. Cicolani

Ames Research Center

Moffett Field, Calif. 94035

NATIONAL AERONAUTICS AND SPACE ADMINISTRATION • WASHINGTON, D. C. • JANUARY 1973

1. Report No.	2. Government Accession No.	3. Recipient's Catalog No.
NASA TN D-7116		

4. Title and Subtitle	5. Report Date
POSITION DETERMINATION ACCURACY FROM THE MICROWAVE LANDING SYSTEM	January 1973
	6. Performing Organization Code
7. Author(s)	8. Performing Organization Report No.
Luigi S. Cicolani	A-4176
	10. Work Unit No.
9. Performing Organization Name and Address	135-19-02-10-00-21
NASA Ames Research Center Moffett Field, California 94035	11. Contract or Grant No.
	13. Type of Report and Period Covered
12. Sponsoring Agency Name and Address	Technical Note
National Aeronautics and Space Administration Washington, D.C. 20546	14. Sponsoring Agency Code

15. Supplementary Notes

16. Abstract

Analysis and results are given for the position determination accuracy obtainable from the microwave landing guidance system. Results are computed for the Radio Technical Commission for Aeronautics SC-117 system configurations D, F, and K, including their corresponding siting arrangements, coverage volumes, and accuracy standards for the azimuth, elevation, and range functions of the microwave system. These configurations correspond to categories I, II, and III flight operational requirements, respectively.

Results are given for the complete coverage of the systems and are related to flight operational requirements for position estimation during flare, glide slope, and general terminal area approaches.

Range rate estimation from range data is also analyzed. The Distance Measuring Equipment accuracy required to meet the range rate estimation standards of SC-117 is determined, and a method of optimizing the range rate estimate is also given.

17. Key Words (Suggested by Author(s))	18. Distribution Statement
Microwave landing system Aircraft terminal area position estimation Aircraft range rate estimation	Unclassified – Unlimited

19. Security Classif. (of this report)	20. Security Classif. (of this page)	21. No. of Pages	22. Price*
Unclassified	Unclassified	41	$3.00

* For sale by the National Technical Information Service, Springfield, Virginia 22151

TABLE OF CONTENTS

SYMBOLS

AZ	azimuth angle; angle between aircraft and runway center plane, measured at the azimuth antenna
d	distance from DME antenna to aircraft
EL, EL_1, EL_2	elevation angle; angle between aircraft and horizontal plane measured at the elevation antenna; EL_1, EL_2 refer, respectively, to the glide slope and flare elevation antennas
L	longitudinal distance between AZ and EL_1 antennas, $x_A - x_E$
L_A, L_E	longitudinal distance from AZ and EL antennas, respectively, to the aircraft; $x_A - x$, $x_E - x$
$\mathbf{R}$	position vector from origin of the runway coordinate frame, which is on the runway at the glide-slope base
(x,y,z)	Cartesian coordinates of $\mathbf{R}$, in runway coordinate frame
(x_A, y_A, z_A)	Cartesian coordinates of AZ and EL antenna locations
(x_E, y_E, z_E)	
ψ	aircraft elevation angle, measured at the AZ antenna site
σ	RMS value
$(\hat{})$	estimated value of ( )
$(\tilde{})$	error in estimated value of ( )

DEFINITIONS AND ABBREVIATIONS

Altitude	as used here, altitude above the origin of the runway coordinates; that is $\|z\|$
Distance from antenna	as used here, x-component of the position vector from the antenna to the aircraft
GS	glide slope
MLS	microwave landing system; referring to the combined azimuth and elevation antennas, the DME, and associated ground and airborne equipment

POSITION DETERMINATION ACCURACY FROM THE MICROWAVE LANDING SYSTEM

Luigi S. Cicolani

Ames Research Center

SUMMARY

Analysis and results are given for the position determination accuracy obtainable from the microwave landing guidance system. Results are computed for the Radio Technical Commission for Aeronautics SC-117 system configurations D, F, and K, including their corresponding siting arrangements, coverage volumes, and accuracy standards for the azimuth, elevation, and range functions of the microwave system. These configurations correspond to categories I, II, and III flight operational requirements, respectively.

Results are given for the complete coverage of the systems and are related to flight operational requirements for position estimation during flare, glide slope, and general terminal area approaches.

Range rate estimation from range data is also analyzed. The Distance Measuring Equipment accuracy required to meet the range rate estimation standards of SC-117 is determined, and a method of optimizing the range rate estimate is also given.

INTRODUCTION

The microwave landing guidance system (MLS) consists of azimuth, elevation, and DME antenna systems at the runway and corresponding airborne receiving equipment to provide position and velocity navigation data for terminal area flight operations. Insofar as CTOL operations are concerned, preliminary design and system integration has been carried out by RTCA (ref. 1), including siting arrangements of the ground equipment, volume of coverage and format of the signals, and accuracy standards for the combined ground-based and airborne equipment.

The MLS is one of the important factors in planning (ref. 2) for future terminal area flight operations for military and civilian CTOL aircraft, V/STOL aircraft, and all types of airports and STOLports. Navigation data for approach paths, center plane and glide-slope tracking, and decision height altitude are currently obtained from the ILS glide-slope beam, localizer, VORTAC, DME, markers, altimeters, etc. In addition to these functions, the MLS can provide data for automatic landing and for arbitrary flyable paths within its volume of coverage. With suitable accuracy this flexibility in choice of path can then be used for noise abatement throughout the terminal area, and for time and separation control of high density traffic.

This paper examines the position estimation accuracy obtainable from the MLS throughout the coverage and with reference to the requirements of flight operations. The calculations assume

that the aircraft position coordinates relative to the runway are determined from samples of range, azimuth, and elevation, which are available at the output of the receiver and at the accuracy standards specified in reference 1. These standards do not necessarily reflect the performance of existing hardware, but are design criteria that the combined ground and airborne equipment of the MLS are expected to meet. It is also assumed that the data rate is sufficient that position accuracy deterioration between samples is small compared to the estimation accuracy. Within these assumptions, the obtainable position accuracy is independent of the data rate of the system. It is also noted that the specified bias error component for each data type is sufficiently large that little advantage in position accuracy can be obtained by averaging over multiple data samples. Consequently, the results given here are expected to provide reasonably well the position estimation performance of the MLS independent of data rate or method of data processing.

THE MICROWAVE LANDING SYSTEM

Coordinate Frame, Antenna Locations, System Coverage, and Scan Rates

In the analysis, the aircraft position coordinates are given in a right-handed orthogonal coordinate frame with the origin on the runway centerline at the glide-slope base, which, for conventional runways, is about 305 m (1000 ft) forward of the runway threshold. Its z-axis is positive downward along the local gravity vector and the x-axis is along the runway centerline and is positive in the direction of flight of approaching aircraft. In practice, the runway may have small gradients and undulations with respect to the local horizontal plane.

The MLS for conventional airport use consists of azimuth and DME antennas at the stop end of the runway, an elevation antenna at the glide-slope base, and a special elevation antenna forward of the glide-slope base for use during automatic flare and landing operations (see sketch (a)). The antenna system shown is denoted configuration K in reference 1. Lesser configurations of reference 1 are intended for categories I and II operations and omit the EL_2 antenna. Other siting arrangements are also possible, such as colocation of all ground equipment, but these arrangements are not investigated here.

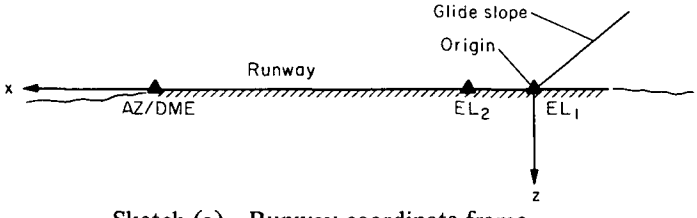

Sketch (a)– Runway coordinate frame and antenna locations.

The azimuth and DME antenna location is denoted by (x_A, y_A, z_A) and the elevation antenna location by (x_E, y_E, z_E). In conventional practice, the glide-slope base will be at about 1000 ft from the threshold as a result of FAA requirements (refs. 3 and 4) for a glide-slope angle in the range 2.5° to 3.0° with beam heights of 15 to 18 m (50 to 60 ft) at the threshold. Consequently, the value of x_A will be in the range of 1800 to 3900 m (6000 to 13,000 ft), depending on runway length. Also, y_A is normally zero, while z_A does not enter the calculations of this report.

The EL_1 antenna will normally be at the glide-slope base, longitudinally, and offset from the runway laterally on the order of 120 to 150 m. The flare antenna EL_2 can be expected to be located at about 600 to 750 m (2000 to 2500 ft) forward of the glide-slope base and thus forward of the touchdown point for most aircraft landing within the FAA touchdown point dispersion

requirements for category III landings (ref. 5). The lateral offsets of the two antennas do not enter the calculations, but the antenna heights must be accounted for, especially during flare where they are of the same order as the accuracy of calculating aircraft altitude and of the difference of the wheelbase to receiving-antenna height. The values of x_{E_1}, z_{E_1}, and z_{E_2} will be taken as zero in the calculations of this report.

The spatial coverage of the MLS differs among several configurations given in reference 1. The coverage for three of these configurations is given in table 1; for this paper, however, interest in the different configurations is based more on their different accuracy standards and intended flight operational use than on details of coverage differences.

TABLE 1.– MLS COVERAGE

RTCA SC-117 config. operational use	D Cat. I	F Cat. II	K Cat. III
Volume of coverage			
DME	3.7-5.6 km (20-30 n.mi.)	3.7-5.6 km	3.7-5.6 km
AZ			
Azimuth	±20°	±20°	±60°
Elevation	0-8°	0-8°	0-20°
Distance	3.7-5.6 km	3.7-5.6 km	3.7-5.6 km
EL_1			
Elevation	1-8°	1-8°	1-20°
Azimuth	±20°	±20°	±60°
Distance	3.7-5.6 km	3.7-5.6 km	3.7-5.6 km
EL_2			
Elevation	– – –	– – –	0-8°
Azimuth	– – –	– – –	±40°
Distance	– – –	– – –	9.3 km (5 n.mi.)
Runway length	2.13 km (7000 ft)	3.66 km (12,000 ft)	4.27 km (14,000 ft)
Minimum guidance height	45.7 km (150 ft)	15.2 km (50 ft)	TD

The required coverage volume is also limited by a 6 km (20,000 ft) altitude ceiling.

The configuration data are illustrated in sketch (b). Note that the boundaries of the *EL* coverage are interior to the *AZ* coverage. Further, an elevation coverage boundary in the ground

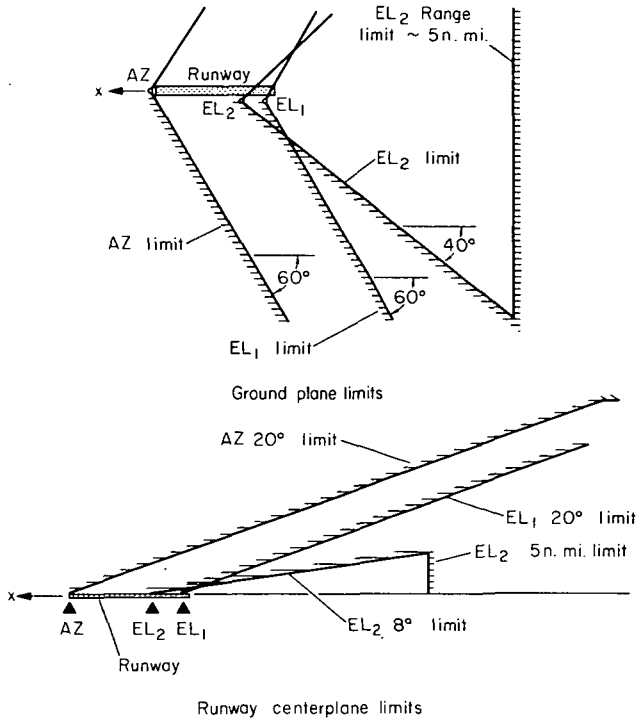

Sketch (b).– Configuration K coverage limits

plane crosses the runway centerline somewhere between the glide-slope base and the threshold, possibly at the threshold for configurations D and F.

The RTCA SC-117 provisional data rates (ref. 1) are: EL_1, 5 Hz; EL_2, 10 Hz; AZ, 5 Hz within ±20° and 2.5 Hz remaining coverage, if any; and DME, 40 Hz. The angle antennas are synchronized so that signals for each function are emitted during different time periods in a fixed sequence. The DME can be independently interrogated at 40/sec. Reference 1 can be consulted for further details.

LGS Data Accuracy Standards

Reference 1 specifies the accuracy standards for the different configurations of the MLS. These standards refer to errors due to all sources in the combined system of ground and airborne equipment; that is, it is the required accuracy with which the values of (d, AZ, EL) are available from the airborne receiver system at the time the signals are received.

Table 2 gives the accuracy standards of reference 1 as RMS (1σ) values. In each case the total RMS bias error (errors that are constant from sample to sample) and RMS random error (errors that are independent from sample to sample) are given along with the total RMS value of the two independent error types. The table specifies the minimum accuracy for systems used in each configuration. These standards, strictly speaking, apply at the location of the minimum guidance height on the approach flight path for each configuration (45.7 m (150 ft), 15.2 m (50 ft), and touchdown for configurations D, F, and K, respectively). Accuracy degradation is permitted at close range to the antenna, and at off-course and long-range locations accuracy degradation is limited to a factor of 2. In this report accuracy loss at close ranges is included in the results, but otherwise the accuracies quoted above are taken as constant throughout the coverage of the MLS for lack of a model of the off-course location dependence of errors.

Errors for the three data types of the MLS are assumed independent of each other. This requires only that they share no significant common source of bias error.

The RMS DME random error is not given in table 2. The range rate estimation error depends on the random component of the DME error, but is independent of the bias component. Thus, the RTCA SC-117 standard (ref. 1) for the random error is that it be compatible with a range rate estimation error of about 3 m/sec (10 ft/sec), obtained by averaging range samples over a period

TABLE 2.– ACCURACY STANDARDS (1σ) FOR RTCA SC-117 CONFIGURATIONS

Configuration operational use	D Cat. I	F Cat. II	K Cat. III
DME			
Bias	91.4 m (300 ft)	30.5 m (100 ft)	6.1 m (20 ft)
Random	*	*	*
Total	91.4 m	30.5 m	6.1 m
AZ			
Bias	2.18×10^{-3} rads	1.57×10^{-3}	0.628×10^{-3}
Random	1.15×10^{-3}	$.575\times10^{-3}$	$.41\times10^{-3}$
Total	2.46×10^{-3}	1.67×10^{-3}	$.741\times10^{-3}$
EL			
Bias	0.872×10^{-3} rads	0.872×10^{-3}	0.872×10^{-3}
Random	1.02×10^{-3}	$.61\times10^{-3}$	$.61\times10^{-3}$
Total	1.35×10^{-3}	1.06×10^{-3}	1.06×10^{-3}

*Random error negligible compared to bias.

of 0.2 sec from DME interrogations at 40/sec. From this it can be calculated (eq. (11b) or (11c)) that the required RMS DME random error is 0.61 m (2 ft) or less, in which case it has negligible effect on the total range measurement error.

The distinction between bias and random errors would enter the performance calculations if multiple samples of the MLS data were averaged over a period of time to improve the position estimate and to estimate velocity. In averaging, the bias component limits the obtainable position accuracy, while velocity accuracy is independent of the bias component. In the MLS accuracy standards (table 2), the bias errors are sufficiently large that little position accuracy improvement is obtained by averaging compared to not averaging. Consequently, averaging methods need not be considered here, nor does the distinction between bias and random error components enter the position accuracy calculations.

The estimation of range rate from range data is discussed in a later section, where the analysis shows the dependence of velocity estimation performance on both random error and the length of the averaging time. Finally, the division into constant and random errors above is simplistic. Bias errors generally drift; if the drift is negligible over the time period the aircraft uses the data type, or compared to the time span over which data is averaged, then that error can be regarded as an unknown bias.

In table 2 the following characteristics of the three configurations are noted. The DME error is almost entirely bias and the accuracy standard varies by an order of magnitude among the three configurations. For azimuth accuracy, the larger error source is a bias, and accuracy deteriorates

by a factor of 3 from configuration K to D. The elevation accuracy standard is the same for configurations K and F, and is degraded by only a factor of 1.3 in configuration D. The RMS bias and random errors are about the same size for elevation angle.

POSITION DETERMINATION AND ACCURACY

The formulations, discussion, and results in this section are organized around the flight operational requirements for navigation data from the MLS. For this purpose, the MLS coverage has been roughly divided into a flare region, final approach region, and terminal area navigation region to reflect the different phases of conventional terminal area approach and landing operations and their corresponding differences in accuracy and data type requirements.

The flare region refers to the runway center plane and vicinity, from the EL_2 antenna out past the runway threshold some distance. This region contains the final part of the glide slope at altitudes of 150 ft or less, and the flare and touchdown maneuver. It is of interest principally in connection with automatic landing using the configuration K flare antenna.

The final approach region refers to the extended runway center plane and vicinity, from threshold out to 15 km (50,000 ft). In this region, aircraft are on conventional straight-in approaches that intercept and track the glide slope down to the decision or alert height, at which point the aircraft is flown VFR, on automatic landing, or on go-round procedure.

The terminal area navigation region is the remainder of the MLS coverage, and contains flight paths leading up to the final approach in the center plane. In current practice flight paths in this region are highly standardized at any one airport, but vary widely among airports so that accuracy throughout this region of coverage is of interest. Future operations designed to control noise and arrival time will utilize more of this region of MLS coverage at any one airport.

Determination of Aircraft Position

The relation between aircraft position in Cartesian coordinates and in the variables of the MLS is given here.

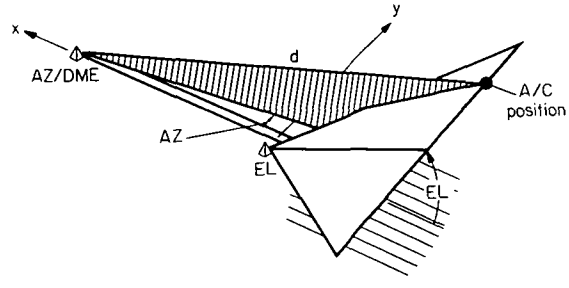

Sketch (c).– Position coordinates.

Each angle antenna rotates on its axis, emitting signals into a narrow depth planar beam. The axis of the azimuth antenna is vertical, and those of the elevation antennas are parallel to the y axis. Consequently, the MLS angle variables are related to the coordinates of the airborne receiving antenna (x,y,z) by (see sketch (c)):

$$\left.\begin{aligned} \tan AZ &= y/L_A \\ \tan EL &= -\frac{z - z_E}{L_E} \end{aligned}\right\} \tag{1}$$

where

$$\left.\begin{aligned} L_A &\equiv x_A - x \\ L_E &\equiv x_E - x \\ L &= x_A - x_E \end{aligned}\right\} \tag{2}$$

The DME transponder is interrogated by the aircraft and a reply is returned, the range from the DME antenna being determined from the round trip time of the interrogation and reply sequence. The range is then

$$d = \sqrt{L_A{}^2 + y^2 + z^2} \tag{3}$$

Reference 1 visualizes a built-in delay in the transponder between reception of the interrogation signal and emission of the reply signal, this delay being calibrated at each runway so that an aircraft at the origin (glide-slope base) receives its reply after 60 μsec. The range tracker then measures the time from this standard delay; consequently, its output is

$$d_1 = \sqrt{L_A{}^2 + y^2 + z^2} - x_A \tag{4}$$

However, the relative locations of the antennas will also be supplied in the MLS signals so that d is readily computed as needed.

Cartesian coordinates of aircraft position– Equations (1) and (3) can be inverted to obtain

$$x = \frac{x_A + x_E \tan^2 EL \cos^2 AZ - \cos AZ \sqrt{d^2 (1 + \tan^2 EL \cos^2 AZ) - L^2 \tan^2 EL}}{1 + \tan^2 EL \cos^2 AZ} \tag{5}$$

The values of y and z can be computed from equations (1) after forming L_A and L_E from the computed value of x. Formulas for y and z in terms of the MLS variables alone are given by

$$y = \sin AZ \frac{L \tan^2 EL \cos AZ + \sqrt{d^2 (1 + \tan^2 EL \cos^2 AZ) - L^2 \tan^2 EL}}{1 + \tan^2 EL \cos^2 AZ}$$

$$z = z_E + \tan EL \frac{L - \cos AZ \sqrt{d^2 (1 + \tan^2 EL \cos^2 AZ) - L^2 \tan^2 EL}}{1 + \tan^2 EL \cos^2 AZ}$$

Small angle approximations– During the final approach and flare, the value of azimuth is nominally zero, in which case equation (5) becomes

$$x = x_A - L \sin^2 EL - \cos EL \sqrt{d^2 - L^2 \tan^2 EL}$$

In addition, for conventional final approaches the elevation angle is 2.5° to 3.0° (ref. 3) beginning at distances at least 9.3 km (5 n.mi.) from the runway so that small angle approximations can be used.

$$x \cong x_A - d = -d_1$$

$$y \cong dAZ = (x_A + d_1)AZ \tag{6}$$

$$z \cong z_E + (L - d)EL = z_E - (x_E - d_1)EL$$

Along the glide slope, the altitude deviation from the glide slope (which is likely to be the preferred glide-slope control variable) can be determined from

$$\Delta z = z - z_{GS} = -L_E(\tan EL - EL_{GS}) \cong -L_E \, \Delta EL$$

The values of (x,y,z) above are the coordinates of the receiving antenna. Where correction to the coordinates of the aircraft center of gravity or wheel base is required, the appropriate correction term must be added to the above solution.

Path Determination Errors

The error in determining **R** by inverting the current values of (d, AZ, EL) depends on the errors $(\tilde{d}, \tilde{AZ}, \tilde{EL})$ with which these variables are measured. The relation is given from the partial derivatives of **R** with respect to the MLS variables:

$$\begin{pmatrix} \tilde{x} \\ \tilde{y} \\ \tilde{z} \end{pmatrix} = \begin{bmatrix} \frac{\partial x}{\partial d} & \frac{\partial x}{\partial AZ} & \frac{\partial x}{\partial EL} \\ -\frac{\partial x}{\partial d}\tan AZ & \frac{LA}{\cos^2 AZ} - \frac{\partial x}{\partial AZ}\tan AZ & -\frac{\partial x}{\partial EL}\tan AZ \\ \frac{\partial x}{\partial d}\tan EL & \frac{\partial x}{\partial AZ}\tan EL & \frac{\partial x}{\partial EL}\tan EL - \frac{L_E}{\cos^2 EL} \end{bmatrix} \begin{pmatrix} \tilde{d} \\ \tilde{AZ} \\ \tilde{EL} \end{pmatrix} \tag{7}$$

This is abbreviated by the notation $\tilde{r} = H_r \tilde{w}$. The partial derivatives in equation (7) are obtained from equation (5). Omitting algebra (see appendix A), these are

$$\frac{\partial x}{\partial d} = -\frac{\cos AZ \sqrt{1 + \tan^2 \psi \cos^2 AZ}}{1 + \tan \psi \tan EL \cos^2 AZ}$$

$$\frac{\partial x}{\partial AZ} = \frac{y}{1 + \tan \psi \tan EL \cos^2 AZ}$$

$$\frac{\partial x}{\partial EL} = \frac{L_E \cos^2 AZ \tan \psi}{\cos^2 EL \, (1 + \tan \psi \tan EL \cos^2 AZ)}$$

where

$$\tan \psi \equiv \frac{-z}{L_A}$$

The error coefficient matrix is then

$$H_r = \frac{1}{1 + \tan \psi \tan EL \cos^2 AZ} \begin{bmatrix} -\cos AZ \sqrt{1 + \tan^2 \psi \cos^2 AZ} & y & L_E \dfrac{\cos^2 AZ \tan \psi}{\cos^2 EL} \\ \sin AZ \sqrt{1 + \tan^2 \psi \cos^2 AZ} & -L_A(1 + \tan \psi \tan EL) & -L_E \dfrac{\cos AZ \sin AZ \tan \psi}{\cos^2 EL} \\ -\tan EL \cos AZ \sqrt{1 + \tan^2 \psi \cos^2 AZ} & y \tan EL & \dfrac{-L_E}{\cos^2 EL} \end{bmatrix} \tag{8a}$$

Approximate error coefficient matrix– In conventional practice (ref. 4) CTOL aircraft flying within the MLS coverage are generally at low altitudes and low elevation angles. Noting that $\psi < EL$ and then neglecting $\tan \psi \tan EL$, $\tan^2 EL$, and $\tan \psi \tan EL \cos^2 AZ$ compared to 1.0, we have

$$H_{r_1} \cong \begin{bmatrix} -\cos AZ & y & L_E \cos^2 AZ \tan \psi \\ \sin AZ & L_A & -L_E \sin AZ \cos AZ \tan \psi \\ -\cos AZ \tan EL & y \tan EL & -L_E \end{bmatrix} \tag{8b}$$

On the final approach and flare, azimuth is nominally zero, and EL and ψ are 3° or less for CTOL aircraft. Evaluating equation (8a) on the nominal path obtain:

$$H_{r_2} \cong \begin{bmatrix} -1 & 0 & L_E \tan \psi \\ 0 & L_A & 0 \\ -\tan EL & 0 & -L_E \end{bmatrix} \tag{8c}$$

Position determination accuracy– The covariance matrix of position determination errors is given by

$$Q_r = H_r Q_w H_r^T \tag{9}$$

where

$$Q_r \equiv E\,[\tilde{r}\tilde{r}^T]$$

$$Q_w \equiv E\,[\tilde{w}\tilde{w}^T]$$

The diagonal elements of Q_r are the variances of x,y,z. The value of Q_w used in the calculations of this report is:

$$Q_w = \text{diag}\,(\sigma_d^2,\ \sigma_{AZ}^2,\ \sigma_{EL}^2) \tag{10}$$

where the values of σ_d, σ_{AZ}, σ_{EL} are as given in table 2 for the RTCA SC-117 configurations of interest. The total error (combined bias and random error) is used in each case. Equations (8), (9), and (10) were used in investigating the obtainable position determination accuracy for various regions of MLS coverage, and for typical flight paths of interest. Results are discussed in the next section.

Formulas for the variances of x,y,z errors can be derived by substitution of equations (8) and (10), into (9). From equation (8a) the exact formulas are

$$\left.\begin{aligned}
\sigma_x &= A\sqrt{\left\{1+\tan^2\psi\cos^2 AZ\left[1+\left(\frac{L_E\,\sigma_{EL}}{\cos EL\,\sigma_d}\right)^2\right]\right\}\cos^2 AZ\,\sigma_d^2 + y^2\,\sigma_{AZ}^2} \\
\sigma_y &= A\sqrt{\left\{1+\tan^2\psi\cos^2 AZ\left[1+\left(\frac{L_E\,\sigma_{EL}}{\cos EL\,\sigma_d}\right)^2\right]\right\}\sin^2 AZ\,\sigma_d^2 + \left(1+\tan\psi\tan EL\right)^2 L_A^2\,\sigma_{AZ}^2} \\
\sigma_z &= A\,L_E\,\sigma_{EL}\sqrt{\cos^{-2} EL + \left[(1+\tan^2\psi\cos^2 AZ)\left(\frac{\cos AZ\,\sigma_d}{L_E\,\sigma_{EL}}\right)^2 + \left(\frac{y\,\sigma_{AZ}}{L_E\,\sigma_{EL}}\right)^2\right]\tan^2 EL}
\end{aligned}\right\} \tag{11a}$$

where

$$A = (1+\tan\psi\tan EL\cos^2 AZ)^{-1}$$

The small elevation angle approximation (8b), applicable to most CTOL flight paths within the MLS coverage, gives

$$\left.\begin{aligned}
\sigma_x &= \sqrt{\left[1 + \tan^2 \psi \cos^2 AZ \left(\frac{L_E \sigma_{EL}}{\sigma_d}\right)^2\right] \cos^2 AZ \, \sigma_d^2 + y^2 \sigma_{AZ}^2} \\
\sigma_y &= \sqrt{L_A^2 \sigma_{AZ}^2 + \left[1 + \tan^2 \psi \cos^2 AZ \left(\frac{L_E \sigma_{EL}}{\sigma_d}\right)^2\right] \sin^2 AZ \, \sigma_d^2} \\
\sigma_z &= L_E \sigma_{EL} \sqrt{1 + \tan^2 EL \left[\cos^2 AZ \left(\frac{\sigma_d}{L_E \sigma_{EL}}\right)^2 + \left(\frac{y \sigma_{AZ}}{L_E \sigma_{EL}}\right)^2\right]}
\end{aligned}\right\} \qquad (11b)$$

The small angle approximation (8c), valid for final approach and flare, gives

$$\left.\begin{aligned}
\sigma_x &= \sqrt{\sigma_d^2 + \tan^2 \psi \, L_E^2 \, \sigma_{EL}^2} \\
\sigma_y &= L_A \, \sigma_{AZ} \\
\sigma_z &= \sqrt{L_E^2 \, \sigma_{EL}^2 + \tan^2 EL \, \sigma_d^2}
\end{aligned}\right\} \qquad (11c)$$

Remarks

In deriving the coordinate inversion equation (5) from which the accuracy equations (11) is obtained, it is assumed that values of $d(t)$, $AZ(t)$, $EL(t)$ are continuously available for inversion. One method of providing these values continuously is the sample-and-hold system (ref. 6). The output of this system is in error because samples of the three variables are received intermittently and nonsimultaneously. This error increases approximately linearly with time during the interval between data receptions and has a step decrease at each reception. The maximum size of this error depends on the combination of data rates and aircraft motion. On the final approach, the values of AZ and EL are nominally held constant. Errors are therefore given by the combination of scan interval and aircraft angle rates arising from random disturbances of the aircraft from its nominal path and are expected to be small. Maximum range rates are on the order of 76 m/sec (250 ft/sec) during final approach, but the DME is interrogated at 40 Hz so that errors of 1.8 m (6 ft) between samples can result. These errors are small, however, compared to the DME measurement accuracy. The actual accuracy of a sample-and-hold system will be poorer at all times than is calculated by equation (11), but the difference is expected to be second order.

The fact that the DME can be interrogated at a substantially higher rate than the angle data is received does not imply that range can be determined to much better accuracy than that given in table 2, say, by averaging all the range samples that can be obtained between receptions of angle data. The DME error is almost entirely bias and cannot be reduced by averaging multiple samples. Similarly, the improvement in position determination accuracy obtainable by sequential data processing of multiple data points is limited by the system bias errors and is not expected to provide accuracies significantly better than those calculated here. Consequently, the results obtained from equations (11) should represent reasonably well the accuracies generally achieved by systems using the MLS as the data source.

RANGE RATE ESTIMATION

The range rate can be estimated by a process equivalent to calculating the time derivative of range, carried out by making a least-squares fit of a straight line through range samples received over a period of time. The accuracy of this estimate will depend on the random errors in the range samples and on the combination of aircraft accelerations and length of the averaging time as discussed in this section.

The RTCA SC-117 requirement for the random DME error (appendix A of ref. 1) is that it be compatible with an RMS range rate error of 3 m/sec (10 ft/sec) when the range rate is obtained from averaging range samples over 0.2 sec. The required RMS random DME error, as calculated in this section, is 0.6 m (2 ft).

In addition, the accuracy of the range rate estimate can be improved by averaging over longer intervals. Alternatively, the range rate standard of 3 m/sec can be met from range samples of RMS random error larger than 0.6 m by averaging over longer intervals. The presence of unmodeled or unknown aircraft accelerations imposes an opposing trend of decreasing accuracy with increasing averaging time, and the two effects combine to limit the achievable range rate accuracy and provide an optimum averaging time.

Analysis

The current range and range rate are computed by fitting a straight line to range samples received during the preceding interval of a given length called the averaging time. Mathematically, the "fit" (least-squares solution) is the straight line that minimizes the sum of the squares of the differences between the straight line and the data. The computations discussed here are based on three assumptions:

Assumptions

1. The aircraft range $d(t)$ is linear with time,

2. The sampling rate is constant, $1/\Delta T$,

3. The sample errors are:

b = bias error; $\quad E[b] = 0, \quad E[b^2] = \sigma_b{}^2$

ϵ = random error; $\quad E[\epsilon] = 0, \quad E[\epsilon^2] = \sigma_r{}^2$

Assumption 1 is inaccurate in the presence of accelerations, $\ddot{d}$. The error involved depends on the averaging time and the level of acceleration. In the present case it is a good approximation for the 0.2-sec interval and for values of $\ddot{d}$ found on final approaches, where a maximum value of about 1 ft/sec^2 is characteristic of aircraft limits. Assumption 2 reflects the expected constant interrogation rate design of the DME receiver, but is slightly inaccurate to the extent that, in practice, some replies are lost. The sample errors are separated into an unknown bias error

(essentially constant over the averaging time) and a random error (independent from sample to sample). Zero mean and constant variances are assumed for both error types.

The estimate of the current range and range rate $(\hat{d}_1, \hat{\dot{d}}_1)$ is obtained by a least-squares fit of a straight line

$$\hat{d}(t) = \hat{d}_1 - \hat{\dot{d}}_1 (t_1 - t) \tag{12}$$

to the data $\{y(t_K), K = 1, \ldots N\}$, where the data are assumed related to the actual aircraft range and range rate $(d_1, \dot{d}_1)$ by

$$y(t_K) = d_1 - \dot{d}_1 (t_1 - t_K) + b + \epsilon_K \tag{13}$$

as illustrated in sketch (d).

The sum of the squares of residuals is

$$S = \sum_{K=1}^{N} (y_K - \hat{d}_K)^2$$

$$= \sum_{K=1}^{N} (y_K - \hat{d}_1 + \hat{\dot{d}}_1 \Delta t_K)^2$$

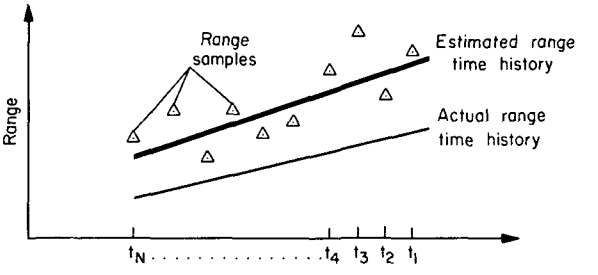

Sketch (d).

where $\Delta t_K = t - t_K = (K-1)\,\Delta T$. The solutions for $(\hat{d}_1, \hat{\dot{d}}_1)$ are found such that S is minimized; that is, they are solutions of

$$\frac{\partial S}{\partial \hat{d}_1} = 0 = \sum_{K=1}^{N} (y_K - \hat{d}_1 + \hat{\dot{d}}_1 \Delta t_K)$$

$$\frac{\partial S}{\partial \hat{\dot{d}}_1} = 0 = \sum_{K=1}^{N} (y_K - \hat{d}_1 + \hat{\dot{d}}_1 \Delta t_K)\,\Delta t_K \tag{14}$$

from which

$$\hat{d}_1 = \frac{2 \sum_{K=1}^{N} y_K (2\,(N+1) - 3K)}{N\,(N+1)} \tag{15}$$

$$\hat{\dot{d}}_1 = \frac{6 \sum_{K=1}^{N} y_K (N + 1 - 2K)}{(N-1)\,N\,(N+1)\,\Delta T} \tag{16}$$

The errors in these solutions are defined as

$$\tilde{d}_1 = \hat{d}_1 - d_1$$

$$\tilde{\dot{d}}_1 = \hat{\dot{d}}_1 - d_1$$

Expressions for these are obtained by substituting equation (13) into (14) and solving for $\tilde{d}_1, \tilde{\dot{d}}_1$:

$$\tilde{d}_1 = b + \frac{2 \sum_{K=1}^{N} \epsilon_K (2(N+1) - 3K)}{N(N+1)}$$

$$\tilde{\dot{d}}_1 = \frac{6 \sum_{K=1}^{N} \epsilon_K (N + 1 - 2K)}{(N-1) N (N+1) \Delta T}$$

From these expressions, obtain

$$\left.\begin{aligned} E[\tilde{d}_1] &= 0 \\ E[\tilde{\dot{d}}_1] &= 0 \\ \sigma_{d_1} &\equiv \sqrt{E[\tilde{d}_1^{\,2}]} = \sqrt{\sigma_b^2 + \sigma_r^2 \frac{2(2N-1)}{N(N+1)}} \\ \sigma_{\dot{d}_1} &\equiv \sqrt{E[\tilde{\dot{d}}_1^{\,2}]} = \frac{\sigma_r}{\Delta T} \sqrt{\frac{12}{(N-1) N (N+1)}} \end{aligned}\right\} \qquad (17)$$

These results show that the range rate error variance is independent of the sample bias, as expected, and decreases with increasing values of N, or with increasing averaging time $(N-1)\Delta T$. For the RTCA standards, appropriate values are

$$\sigma_{\dot{d}_1} = 3.05 \text{ m/sec (10 ft/sec)}$$

$$\Delta T = 1/40 \text{ sec}$$

$$(N-1)\ \Delta T = 0.2 \text{ sec} \quad \text{or} \quad N = 9$$

From equation (17) the required value of σ_r is then

$$\sigma_r = 0.6 \text{ m (2 ft)} \qquad (18)$$

The DME RMS random sample error cannot exceed this value if a range rate accuracy of 3 m/sec is to be achieved at the stated values of sample rate and memory length. From equation (17) it is also seen that range rate accuracy improves indefinitely with increasing N or averaging time.

This trend is limited by the effect of the neglected aircraft accelerations. Receivers of varying complexity are conceivable, up to those that use longer averaging times and update the range rate estimate at each sample reception, and thereby improving accuracy beyond 3 m/sec or achieving 3 m/sec accuracy from DME samples with RMS random errors larger than 0.6 m.

Utilizing equation (17), and the indicated values of σ_r, ΔT, N and the RMS bias errors (6.1 m (20 ft), 30.5 m (100 ft), or 91.4 m (300 ft)) of the DME bias error standards for the three configurations, we can see that the process of averaging the random sample errors has negligible effect on the range accuracy, which is

$$\sigma_{d_1} \cong \sigma_b$$

independent of N. Consequently, there is no advantage to estimating range from the least squares fit (eq. (15)). The purpose of the averaging procedure is to estimate range rate (eq. (16)) and utilize the sensitivity of the range-rate accuracy to the number of samples (eq. (17)) to obtain the desired accuracy.

Optimum Averaging Time

The preceding results considered the range rate accuracy obtained from a least-squares fit of a straight line to N range samples received at a fixed rate. The results showed indefinitely improving accuracy with increasing memory length. This result was based on the assumption that the aircraft range is unaccelerated. In practice, the existence of range accelerations unmodeled by the straight line counters this trend and limits the achievable accuracy. A corresponding optimum memory length, which maximizes the range rate estimation accuracy, can be determined.

Here, the accuracy of a least-squares straight-line fit to range samples is calculated assuming that aircraft range acceleration, $\ddot{d}(t)$, is constant.

The results will be valid on the final approach, where aircraft range deceleration is normally held constant and has a maximum value of 0.03 to 0.05 g (1 to 1.5 ft/sec^2). Away from the straight-in final approach as, for example, during a standard turn of 5.6 km radius, 3°/sec angle rate, and 60 to 90 m/sec air speed, the range deceleration can be an order of magnitude greater than 0.03 g and sinusoidal in time. In these cases the assumed constant acceleration provides a conservative result for the actual accuracy.

In view of the above assumption, the samples are related to aircraft motion by

$$y_k = d_1 - \dot{d}_1 \, \Delta t_k - \ddot{d}_1 \, \Delta t_k^2 + b + \epsilon_k \tag{19}$$

Equations (15) and (16) again apply as the solutions for $\hat{d}_1$, $\hat{\dot{d}}_1$ from the received data. The errors are now found by substituting equation (19) into (14), hence:

$$\tilde{d}_1 = \frac{6 \sum_{K=1}^{N} \epsilon_K (N + 1 - 2K)}{(N-1) N (N+1) \Delta T} + \ddot{d} \frac{(N-1) \Delta T}{2} \tag{20}$$

The range rate estimate is now biased

$$E[\tilde{\dot{d}}_1] = \frac{\ddot{d}(N-1)\Delta T}{2}$$

and has RMS value

$$M_{\dot{d}_1} \equiv \sqrt{E[\tilde{\dot{d}}_1^{\,2}]} = \sqrt{\left(\frac{6r}{\Delta T}\right)^2 \frac{12}{(N-1)N(N+1)} + \dddot{d}^2 \left(\frac{(N-1)\Delta T}{2}\right)^2} \tag{21}$$

This result includes the case of $\ddot{d} = 0$ (eq. (17)).

The value of N that minimizes $M_{\dot{d}_1}$ is found to be

$$N^* = \frac{1}{\Delta T}\left(72\,\frac{\Delta T \sigma_r^2}{\ddot{d}^2}\right)^{1/5}$$

Equivalently, the optimum averaging time is

$$T^* \cong N^*\,\Delta T = \left(72\,\Delta T\,\frac{\sigma_r^2}{\ddot{d}^2}\right)^{1/5} \tag{22}$$

The corresponding minimum value of MS range rate error is

$$M^*_{\dot{d}_1} = \sqrt{\frac{5}{2}}\left[\sqrt{\frac{2}{3}}\,\sigma_r^2\,\dddot{d}^3\,\Delta T\right]^{1/5} \tag{23}$$

Note that the approximation, $N^* >> 1.0$ was used in both equations (22) and (23).

The optimum RMS error results from a compromise between the two terms in equation (21). The first term is due to the random measurement noise and decreases with increasing averaging time. The second term is due to the unmodeled constant acceleration and increases with increasing averaging time – that is, with the length of time over which one attempts to fit a straight line to an accelerated curve.

The optimum averaging time and corresponding minimum RMS range rate error are shown in figure 1 as a function of acceleration for the MLS case (σ_r = 0.6 m, data rate = 40/sec). At a deceleration of 0.03 g, a range rate accuracy of 0.3 m/sec is achieved for an averaging time of 1.5 sec.

Equation (21) is plotted in figure 2 where the range rate accuracy is given as a function of the number of samples averaged. Curves are shown for various constant values of range acceleration, and the two figures are for DME RMS random errors of 0.6 m and 3 m (10 ft), respectively.

At low values of $|\ddot{d}|$ (less than 0.1 g) as during final approach or constant range turns around the DME transponder, figure 2(a) (the MLS case) shows optimum averaging times of 1 sec or greater and corresponding range rate accuracy of 0.6 m/sec or less. If the averaging time is set at

0.2 sec, as specified for the SC-117 standards, then the range rate accuracy in figure 2(a) is 3 m/sec independent of deceleration. If the DME random error σ_r degrades to 3 m (10 ft) (fig. 2(b)), the accuracy degrades to 15 m/sec (50 ft/sec) at the 0.2 sec averaging time, but can be improved by an order of magnitude to 1.5 m/sec or better by increasing the averaging time to 1 to 2 sec.

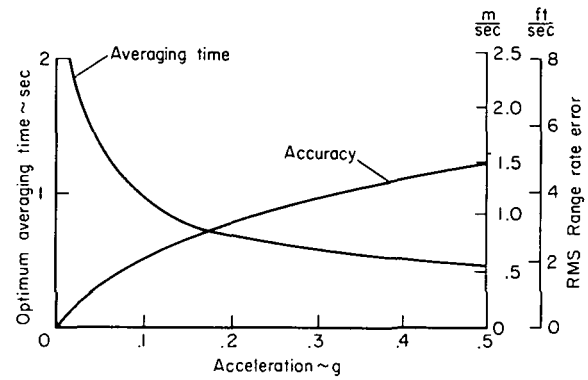

Figure 1.– Optimum averaging time and accuracy (σ_r = 0.6 m, sample rate = 40 Hz).

High values of $|\ddot{d}|$ (up to 0.5 g) can occur during aircraft turns flown in holding patterns and at various points in the terminal area. During such turns $\ddot{d}$ is sinusoidal, rather than constant, with time. Nevertheless, the figures are applicable as follows. If $|\ddot{d}|_{max}$ is the maximum acceleration magnitude during the averaging time, then the accuracy results calculated for

$$\ddot{d}(t) = |\ddot{d}|_{max}$$

are a conservative bound on the actual accuracy. Thus, the curves of figure 2 are conservative if $\ddot{d}$ is taken to be the maximum actual range acceleration during the averaging time.

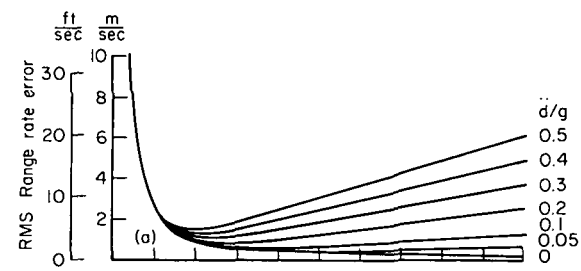

(a) σ_r = 0.6 m, sample rate = 40 Hz.

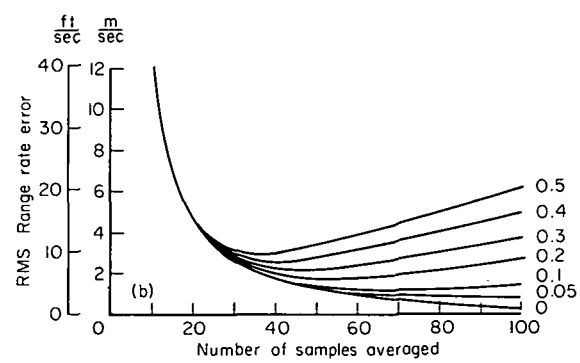

(b) σ_r = 3 m, sample rate = 40 Hz.

Figure 2.– Effects of memory length, acceleration, and sample errors on range-rate accuracy.

At high values of $|\ddot{d}|$ the optimum averaging time is more pronounced and the best obtainable accuracies are poorer than at low accelerations. Figure 2(a) shows that accuracies of 1.5 m/sec or better are achieved with an averaging time of 0.5 sec, and for all accelerations up to 0.5 g. If averaging time is decreased below 0.5 sec, accuracy deteriorates at all accelerations. If averaging time is increased beyond 0.5 sec, accuracy degrades at high accelerations and improves for low accelerations. From figure 2(b), in which σ_r = 3 m, similar conclusions apply at a memory length of 1 sec, at which accuracies are 3 m/sec or better at all accelerations up to 0.5 g.

Remarks

If the range-rate accuracy is to be optimized with respect to averaging times, some flexibility in the choice of averaging time must be available in the hardware used to implement the range rate estimation. If the implemented estimation scheme consists of estimating the range rate (eq. (16)) once every averaging period and holding this value until the end of the next period, a tradeoff occurs between single-estimate accuracy and frequency of providing new estimates. However, if an algorithm can be provided in which the range rate estimate is updated with each reception of a range sample and based on the range samples received during the most recent interval whose length is the selected averaging time, the range-rate estimation frequency is the same as the range data rate and the averaging time can be selected independent of this frequency.

Finally, the least-squares fit method of estimating range rate can be generalized to the three-dimensional problem of estimating aircraft velocity from samples of (AZ, EL, d) obtained from the MLS. As above an optimum averaging time occurs. The formulation will be considerably more complex, involving the transformation from (AZ, EL, d) to Cartesian coordinates, different data rates, and the general limits of aircraft accelerations within the terminal area. In addition, efficient algorithms for limited memory data processing require further research.

The above scheme seeks to optimize the estimation of velocity from the position data provided by the MLS. An analysis is beyond the scope of this paper. An alternate scheme is to provide a generalized complimentary filter in which the MLS position data is combined with acceleration data from an on-board INS or strapdown inertial system. In this case estimation performance will be much less dependent on MLS data rates and averaging time.

DISCUSSION AND RESULTS

The formulas for RMS errors derived in the preceding section were used to calculate the position determination accuracy obtainable from the MLS. The results are discussed separately for the flare region, final approach region, and terminal area navigation region. This is a convenient division of the MLS coverage into regions containing the various segments of standard terminal area landing flight operations and for which navigation data and accuracy requirements differ.

Flare Region Accuracy

Flight paths– The final portion of the flight path consists of the last part of the glide slope and a flare out from the glide slope to touchdown, as shown in sketch (e). In the flare region the source of elevation angle data is the EL_2 antenna, which is intended for automatic flare and touchdown in category III operations.

For purposes of this section, the flare region is limited to that part of the MLS coverage within

$$z \leqslant 45 \text{ m} \qquad L_E \leqslant 1.8 \text{ km} \qquad y \cong 0$$

where L_E is the distance along the x-axis from the EL_2 antenna. In practice (ref. 3) the glide-slope angle is in the range of 2.50° to 3.00° and the required beam height at the runway threshold is 15 to 18 m. Consequently, the threshold is about 300 m from the glide-slope base. The EL_2 antenna is expected to be about 600 to 750 m forward of the glide slope, and hence forward of the touchdown point for most aircraft landing within the category IIIa dispersion criteria.

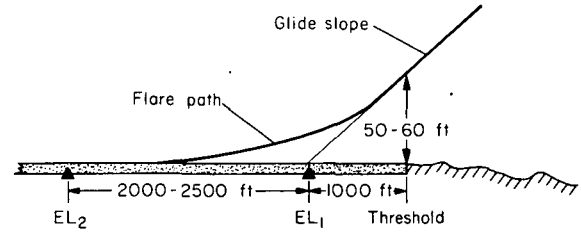

Flare region and flight path

Sketch (e).– Flare region and flight path.

The nominal flare path for automatic landing (ref. 7) is the exponential flare, for which (open-loop) formulas for the wheel-base trajectory are

$$z = \tau\,(\dot{z}_F - \dot{z}_I e^{-t/\tau})$$

$$x = x_I + Vt$$

$$\tau \equiv -z_I/(\dot{z}_I - \dot{z}_F)$$

The subscripts I and F refer to initial and final values on the flare maneuver. Flare initiation occurs at wheel-base altitudes of 9 to 15 m. The design touchdown sink rate is 0.46 to 0.61 m/sec (1.5 to 2.0 ft/sec) usually, and approach air speeds (V) for CTOL aircraft are in the range of 60 to 75 m/sec (200 to 250 ft/sec).

Accuracy results– The RMS position determination errors for this region are given by equation (11c). In the formula for σ_X the elevation error contribution is negligible for the given configuration K accuracies and antenna distances, L_E. The results are then

$$\sigma x \cong \sigma_d$$

$$\sigma y = L_A\,\sigma_{AZ} \tag{25}$$

$$\sigma z \cong \sqrt{L_E^2\,\sigma_{EL}^2 + \tan^2 EL\,\sigma_d^2}$$

The accuracy in determining x depends only on the DME accuracy;

$$6x = 20 \text{ ft}$$

and this is a bias error.

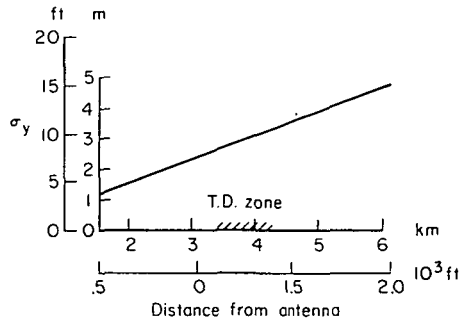

Figure 3.– y determination accuracy – flare region, configuration K.

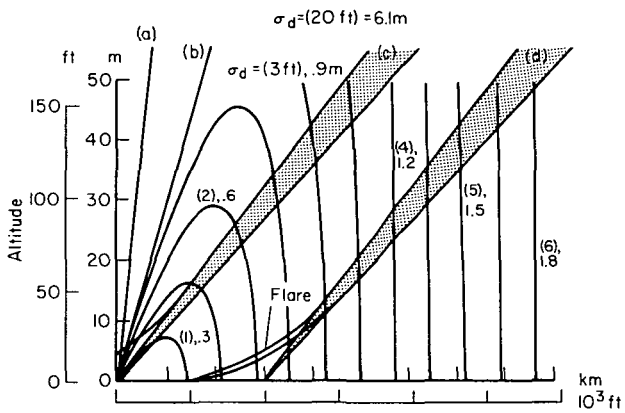

(a) Configuration K

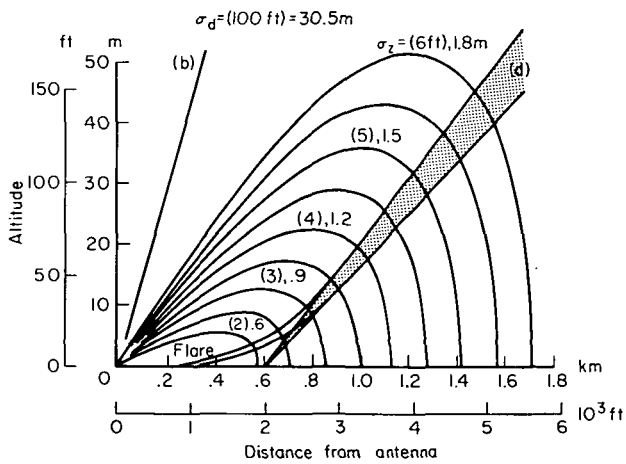

(b) σ_d = 30.5 m (100 ft)

Figure 4.– Altitude estimation accuracy in the flare region.

NOTES: (a) 20° EL_1 coverage limit
(b) 8° EL_2 limit
(c) Glide slope relative to EL_1
(d) Glide slope relative to EL_2

For y, accuracy depends on azimuth measurement accuracy and the location of the azimuth antenna. Results for σ_y are shown in figure 3. For configuration K the first 900 m of runway (touchdown zone) is at distances 3.3 to 4.3 km (11,000 to 14,000 ft) from the antenna. The corresponding RMS error is 2.4 to 3 m or less than 10 percent of the currently standard runway widths of 45 to 60 m (150 or 200 ft).

For automatic flare and landing, the requirements for altitude and altitude rate determination accuracy are the most stringent among the three coordinates. Altitude accuracy (eq. (25)) depends on both DME and EL_2 accuracy and the location of the EL_2 antenna. Plots of accuracy are given in figure 4, in the form of lines of constant σ_z, for both configurations K (fig. 4(a)) and F (fig. 4(b)) accuracies. Although only configuration K is intended for flare region use the plot for configuration F accuracy is provided to show the effect of degrading DME accuracy from 6.1 to 30 m RMS error.

The region of EL_2 coverage utilized by CTOL aircraft is shown in figure 4 by superimposing flight paths of glide angle 2.5° to 3.0° with the base at 600 m from the antenna. At altitudes below 30 m (100 ft) on these flight paths, the RMS altitude determination error is 1.5 m (5 ft) or better for both configuration K and the degraded DME case. For configuration K, these flight paths are located relative to the antenna in an area where the DME error has insignificant effect on the altitude accuracy so that

$$\sigma_z \cong L_E \, \sigma_{EL}$$

If the flight path is "optimized" so that the RMS altitude error is

minimized at each altitude, the "flight path" would be

$$L_E = \sqrt{\frac{\sigma_d}{\sigma_{EL}}}\,|z|^{1/2}$$

which is a line drawn through the peaks of the constant σ_Z curves of figure 4. For configuration K (fig. 4(a)) the RMS error on the standard flight path is about twice the minimum at each altitude. However, the flight path cannot practicably be moved close to the optimum path because of the touchdown dispersion allowances, which place a lower limit on the distance between the glide-slope base and flare antenna. Conversely, the antenna cannot be moved farther away from the glide-slope base without reducing the altitude accuracy during flare.

When configuration F DME is used (fig. 4(b)) the standard flight paths are close to the optimum location. The relative importance of the elevation and DME measurement errors on altitude accuracy differs in the two cases; in figure 4(b) the two sources contribute about equally to the altitude error (they are equal contributors, statistically, on the optimum path), while for configuration K, the DME contribution is negligible.

Some comparisons for the flare region altitude accuracy are made in figure 5, where σ_Z is plotted versus position along the runway centerline and for CTOL flight paths. Results obtained when the EL_2 antenna was used with configurations F and K DME are shown, and it is seen that, from threshold to touchdown, little accuracy loss results from degrading the DME. This insensitivity of altitude determination accuracy to changes in DME accuracy is due to the change in relative location of the standard and optimum paths as DME accuracy is changed. Further deterioration in DME accuracy would have a more pronounced effect on altitude accuracy than seen in figure 5.

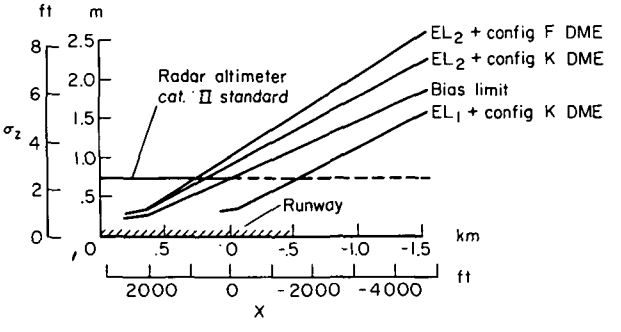

Figure 5.– Flare region altitude accuracy comparisons.

The configuration K results are also compared in figure 5 with the radar altimeter standard for category II equipment (ref. 3, appendix 1). This standard can be interpreted here as the accuracy criterion for decision height measurement. The required altitude determination accuracy during autoflare is expected to be at least as stringent. Configuration K meets or exceeds this standard forward of about 122 m from the glide-slope base, where wheel-base altitude is about 6 m. In addition, approximate smoothing of the MLS data, as is required for sink rate estimation, can improve the altitude estimate somewhat. The potential improvement is limited by the DME and EL_2 bias errors; this limit is shown in figure 5, where it is seen that the available improvement from smoothing is not great.

Both EL_1 and EL_2 signals are simultaneously available for altitude determination up to the boundary of the EL_1 coverage over the runway and out to the 5 n.mi. range of the EL_2 signal. Flare region accuracy using EL_1 data can be determined in figure 4(a) by superimposing the CTOL glide paths with base at the origin. Results are compared with EL_2 usage in figure 5, where

it is seen that, within its region of coverage, EL_1 usage provides twice the accuracy and exceeds the category II altimeter standard within 700 m of the glide-slope base.

Simultaneous use of EL_1 and EL_2 data is conceivable, and this would increase elevation data rate to 15/sec throughout the glide slope should this prove desirable. In addition, values of (x, z, or Δz) can be computed in a novel manner from the two elevation angles and the distance between antennas, but this computation has inferior accuracy.

Final Approach Region Accuracy

The final approach region refers to the centerplane ($AZ = 0$) between runway threshold and 15 km from the threshold.

Flight paths– Conventional CTOL final approaches consist of a constant altitude path until glide-slope intercept and a glide slope down to a minimum decision or alert height, following which the aircraft is flown VFR or an automatic landing in the case of category III. Decision heights are 45.72 m (150 ft) and 30.48 m (100 ft) for categories I and II, respectively, and an alert height is to be specified for category III (ref. 5). Glide slopes are 2.5° to 3°, depending on airport and runway (ref. 4). Glide-slope intercept occurs at 9 km from the runway or beyond. Aircraft altitudes are under 1 km generally throughout this region.

Proposed future operations include two-segment noise abatement approaches in which a steep (6°) glide is flown until intercept (at 120 m altitude or above) with the standard glide slope. (The region used by conventional and two-segment approaches is shown in figure 7 along with the MLS coverage limits.)

Glide-slope accuracy– In tracking the glide slope we can use as the feedback variable either the angle deviation or the altitude deviation from the desired glide slope. The angle deviation accuracy is σ_{EL}. The linear deviation from the glide slope is

$$\Delta z = z - z_{GS} = L_E (\tan EL - \tan EL_{GS}) \cong L_E \, \Delta EL$$

from which

$$\sigma_{\Delta z} \cong L_E \, \sigma_{EL} \sqrt{1 + \left(\frac{\sigma_d \, \Delta EL}{L_E \, \sigma_{EL}} \right)^2} = L_E \, \sigma_{EL} \sqrt{1 + \left(\frac{\sigma_d \, \Delta z}{L_E^2 \, \sigma_{EL}} \right)^2}$$

The DME error appears in a second-order term with the glide-slope deviation, ΔZ. If the aircraft is on the nominal path ($\Delta Z = 0$), there is no effect of DME error on the accuracy, but otherwise a significant effect can appear at low values of L_E.

Glide-slope deviation accuracy is shown below in figure 6(a). The scale is expanded in the vicinity of the threshold and curves are given for both the nominal path and for $\Delta Z = 7.6$ m (25 ft). The effect of the DME at off-path locations is minor beyond threshold and disappears rapidly with distance from the antenna. Configurations F and K provide nearly identical performance, with RMS errors of 1.5 m or better in the final portion of the glide slope below 60 m altitude. Configuration D is only slightly poorer in performance.

Position accuracy– From equation (11a) the RMS position errors are

$$\sigma_x = \sigma_d \sqrt{1 + \tan^2 \psi \left[1 + \left(\frac{L_E \sigma_{EL}}{\cos EL \, \sigma_d}\right)^2\right]} \Big/ A$$

$$\sigma_y = L_A \sigma_{AZ}$$

$$\sigma_z = \sqrt{\left(\frac{L_E \sigma_{EL}}{\cos EL}\right)^2 + \left(\frac{\tan EL}{\cos \psi}\right)^2 \sigma_d^2} \Big/ A$$

$$A \cong 1 + \tan \psi \tan EL$$

The x-determination accuracy is well approximated by

$$\sigma_x \cong \sigma_d$$

everywhere in the final approach region except at altitudes above 3 km for configuration K. Consequently, the RMS x error is 6.1 m, 30.48 m, or 91.44 m for configurations K, F, and D, respectively, and this is bias error.

The y-determination accuracy depends only on azimuth measurement accuracy and increases linearly with distance from the antenna. Some values of interest are given in table 3.

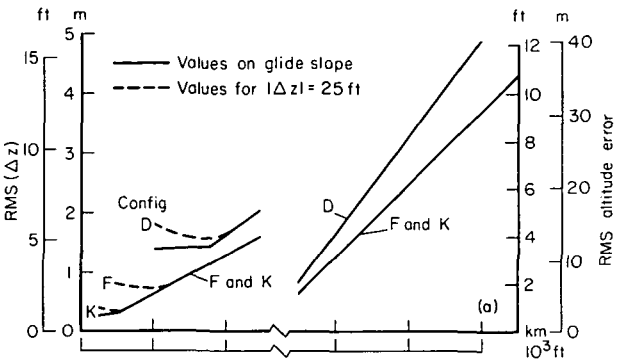

(a) Glide-slope deviation accuracy

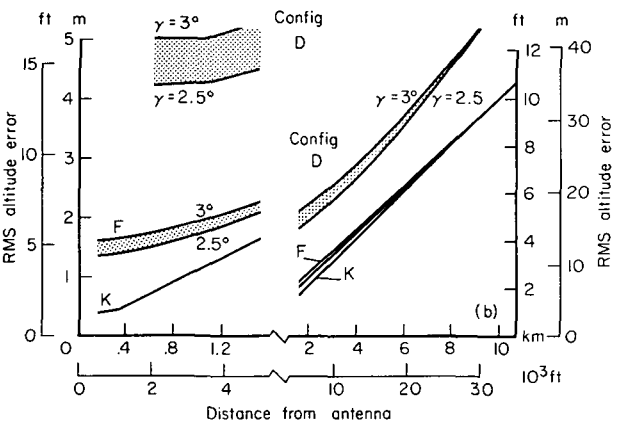

(b) Altitude accuracy

Figure 6.– Glide-slope deviation accuracy and altitude accuracy.

TABLE 3.– VALUES OF σ_y, FINAL APPROACH

SC-117 configuration x_A	K 4 km	F 3.35 km	D 1.8 km
Threshold (x = 1000 ft)	3 m 10 ft	6.1 m 20 ft	5.2 m 17 ft
Outermarker (x = 9 km)	9.7 m 32 ft	21 m 70 ft	28 m 91 ft
x = 18 km	14 m 47 ft	31 m 102 ft	42 m 138 ft

The altitude determination accuracy along standard glide paths is shown in figure 6(b). These results are well approximated by equation (11c).

$$\sigma_z = \sqrt{L_E{}^2 \, \sigma_{EL}{}^2 + \tan^2 EL \, \sigma_d{}^2}$$

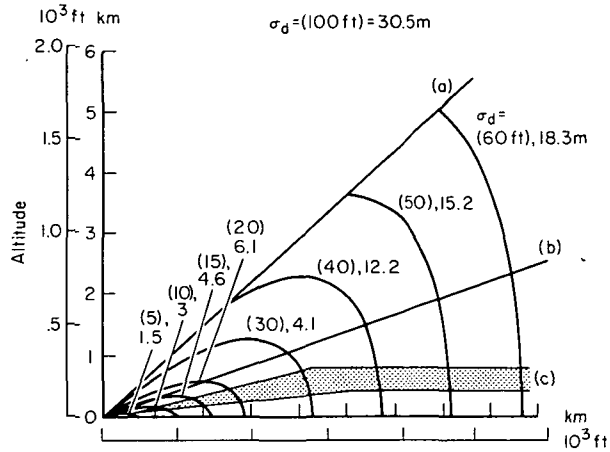

(a) Configuration K

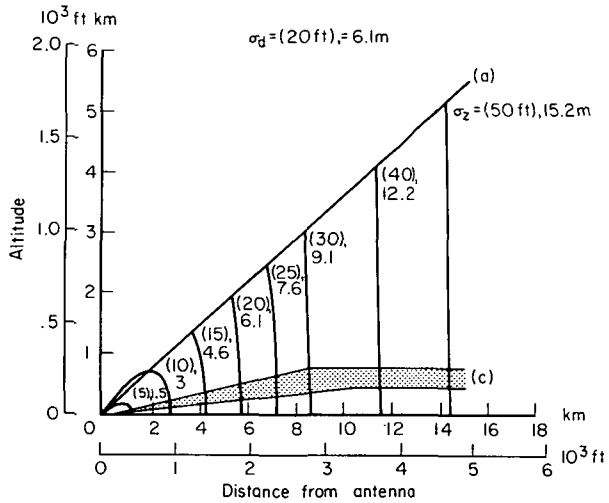

(b) Configuration F

Figure 7.– Altitude estimation accuracy in the final approach region.

NOTES: (a) *EL* coverage limit, configuration K
(b) *EL* coverage limit, configuration F
(c) Region of CTOL and two-segment approach paths

Except in the vicinity of threshold, the principal error source is the elevation angle error and performance is the same as for determining glide-slope deviation. In the vicinity of threshold where the decision height is to be measured, the DME contributes significantly to the altitude error for configurations F and D, as previously discussed. Altitude accuracy within 1.2 km (4000 ft) of the antenna and at the alert and decision heights is 1.2 m (4 ft) or better for configuration K (category III), 1.5 to 2.1 m (5 to 7 ft) for F (category II), and 4.2 to 5.2 m (14 to 17 ft) for D (category III). At higher glide slope angles the DME error has a more pronounced effect on decision height determination accuracy, and on the proposed 7.5° STOL glide path it is the dominating error source.

Finally the altitude determination accuracy throughout the final approach region for configurations F and K are shown in figure 7. The subregion containing standard CTOL glide slopes and two-segment approaches is superimposed on these figures. Accuracy for this subregion depends only on the elevation error ($\sigma_z \cong L_E \sigma_{EL}$) except near threshold as discussed above. Preformance is similar for the three configurations since roughly similar elevation accuracy standards have been specified, with 15 to 21 m (50 to 70 ft) RMS error at 15 km from the antenna. This figure is 2 to 5 percent of nominal aircraft altitudes at this point.

Terminal Area Navigation Region

This region refers to the MLS coverage other than the center plane regions of specialized flight operations and corresponding stringent accuracy requirements discussed previously.

Flight paths– In the terminal area, within 3.7 to 5.6 km (20 to 30 n. mi.) of the runway, flight paths are highly restricted geometrically at any one airport, but the standardized paths vary

among airports so that position determination accuracy throughout the MLS is of interest relative to current operations. In addition, future operations designed to control high density traffic and noise distribution are expected to utilize much of the available terminal area MLS coverage at any one airport.

In this section accuracy results are given for two representative flight paths; the first is a curved approach to the glide-slope intercept and the second approximates the Woodside VORTAC approach to San Francisco International Airport. The coverage and antenna siting of configuration K are assumed in all calculations, although results are given for the accuracy standards of configurations D, F, and K. It is noted that the accuracy deterioration at off-course locations permitted by reference 1 standards is not included in these results for lack of a suitable model. The permitted deterioration is limited to a factor of 2.0.

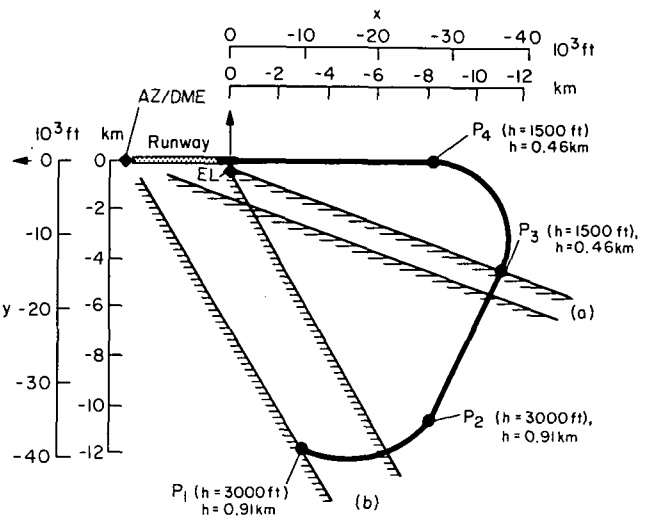

Figure 8. Example terminal area approach path.

NOTES: (a) Configurations F and D, *AZ* and *EL* coverage limits.
(b) Configuration K, *AZ* and *EL* coverage limits.

Accuracy results– The first flight path is a curved approach to the glide-slope intercept as shown in figure 8. It consists of a sequence of constant altitude turns and straight-line paths between waypoints. It remains within 15 km of the origin through and enters the MLS coverage at an altitude of 0.91 km (3000 ft) and elevation angle of 14.5°.

Position determination accuracy is given in figure 9. The independent varable in this figure is path length, beginning from entry into the MLS coverage and ending at touchdown. The major error relationships are approximated by

$$\sigma_x \cong \sqrt{\cos^2 AZ\ \sigma_d^2 + y^2\ \sigma_{AZ}^2}$$

$$\sigma_y \cong \sqrt{\sin^2 AZ\ \sigma_d^2 + L_A^2\ \sigma_{AZ}^2}$$

$$\sigma_z \cong L_E\ \sigma_{EL}/\cos EL$$

Accuracy for the horizontal plane coordinates (x,y) is determined by DME and azimuth accuracy, while altitude accuracy is determined by elevation accuracy. In and near the center plane the approximate relations simplify further to

$$\sigma_x \cong \sigma_d,$$

$$\sigma_y \cong L_A\ \sigma_{AZ},$$

$$\sigma_z \cong L_E\ \sigma_{EL}$$

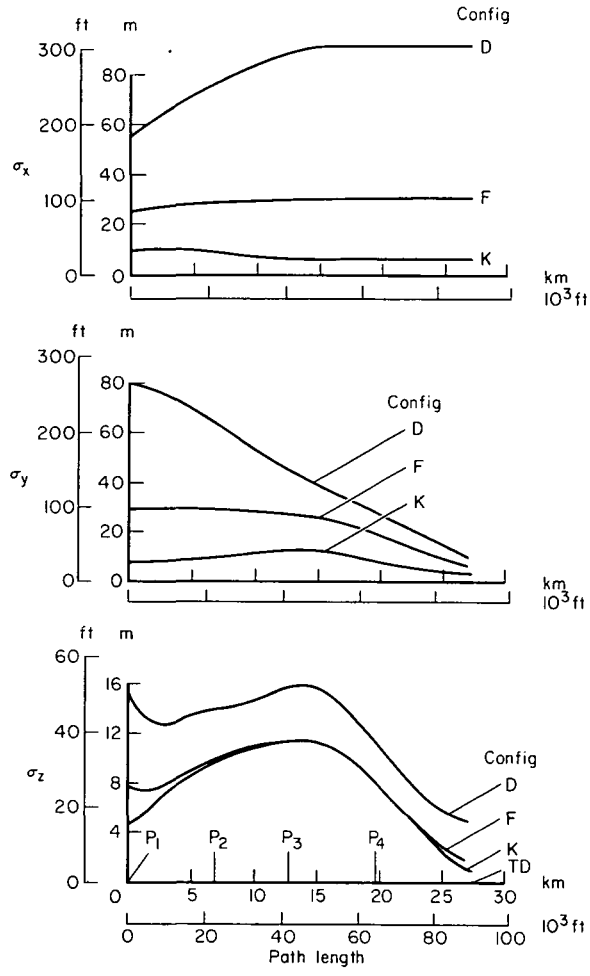

Figure 9.— Position estimation accuracy for example approach path.

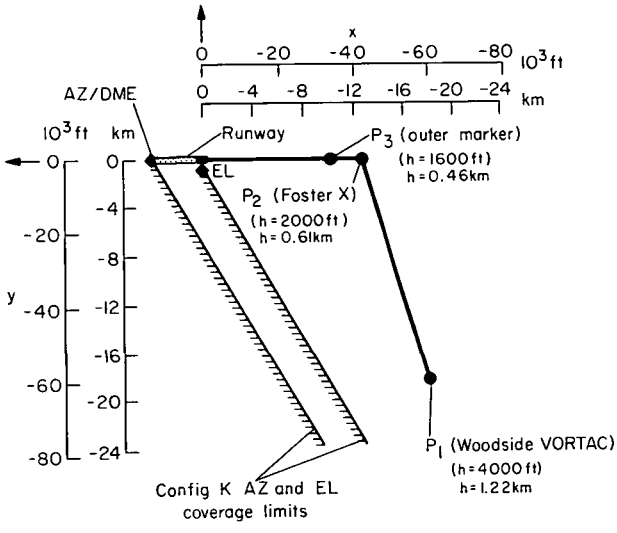

Figure 10.— Example terminal area approach plan.

as discussed earlier for the final approach region. As can be seen in figure 9, the DME error influences altitude accuracy somewhat initially, due to high elevation angle, and near touchdown, as discussed earlier.

The configuration intended for the most comprehensive ATC service is configuration K, which can be seen to provide excellent x, y accuracy — 12 km (40 ft) or better — throughout this flight path. The altitude accuracy variability is due to the increasing and decreasing time history of the x coordinate (L_E), and accuracy is again 12 m at worst for this flight path. Both y and z accuracy improve with decreasing distance to touchdown, while σ_x reaches the DME bias error limit of 6 m (20 ft) as the aircraft arrives in the center plane.

Comparison of results for the three configurations (without regard to coverage limits) shows that the x and y accuracy deteriorates due to deterioration of DME accuracy bv more than an order of magnitude, and deterioration of azimuth accuracy by a factor of 2. The altitude accuracy varies little between configurations K and F, except near touchdown, as expected, but shows poorer performance for configuration D due to the degraded elevation accuracy.

The second flight path case (fig. 10) is approximated simply as two straight lines beginning over Woodside VORTAC at 1.2 km altitude, at azimuth of 41.3°, and at a distance of 44 km from the origin.

Position determination accuracy is given in figure 11(a). The major error relationships are as stated for the first case above. Increase RMS errors in x,y,z are seen prior to glide-slope intercept compared to the preceding case due to the larger distances from the EL_1 and DME antennas. For configuration k, accuracy for (x,y) is 15 m or better throughout, and 18 m at worse for altitude.

Relative deterioration in accuracy among the three configurations shows the same characteristics noted in the preceding case.

Finally, digital filtering of the MLS data can be expected to improve position determination accuracy over that shown in figure 11(a), as well as estimate velocity. The potential improvement in position accuracy is limited by the system biases. Figure 11(b) shows the performance resulting from the system bias errors alone. As expected, virtually no improvement occurs for x, very little for y, and somewhat more for altitude, though not to an important degree.

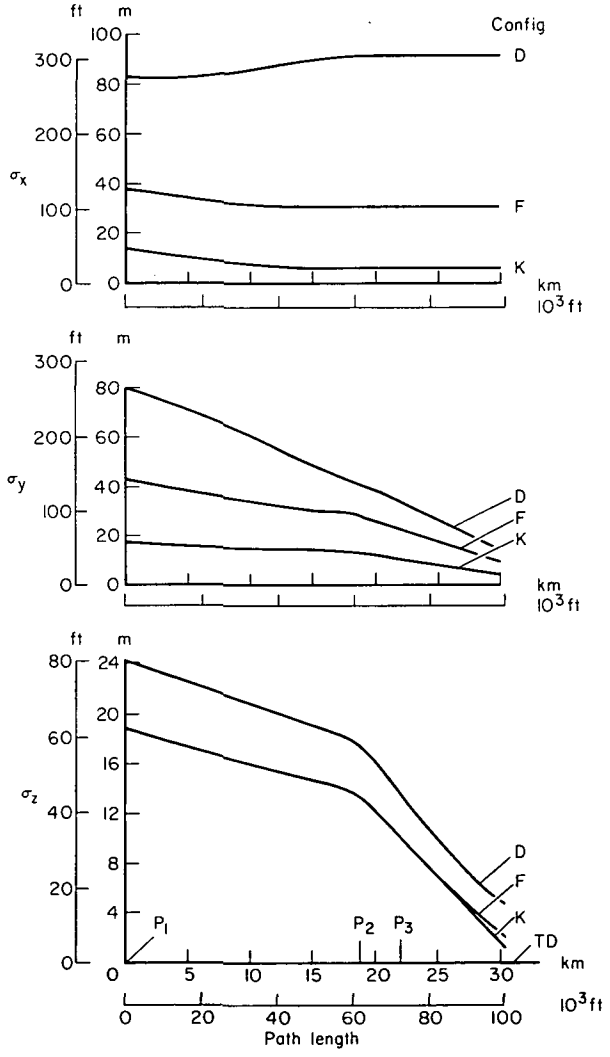

Figure 11(a).– Position estimation accuracy for example approach path.

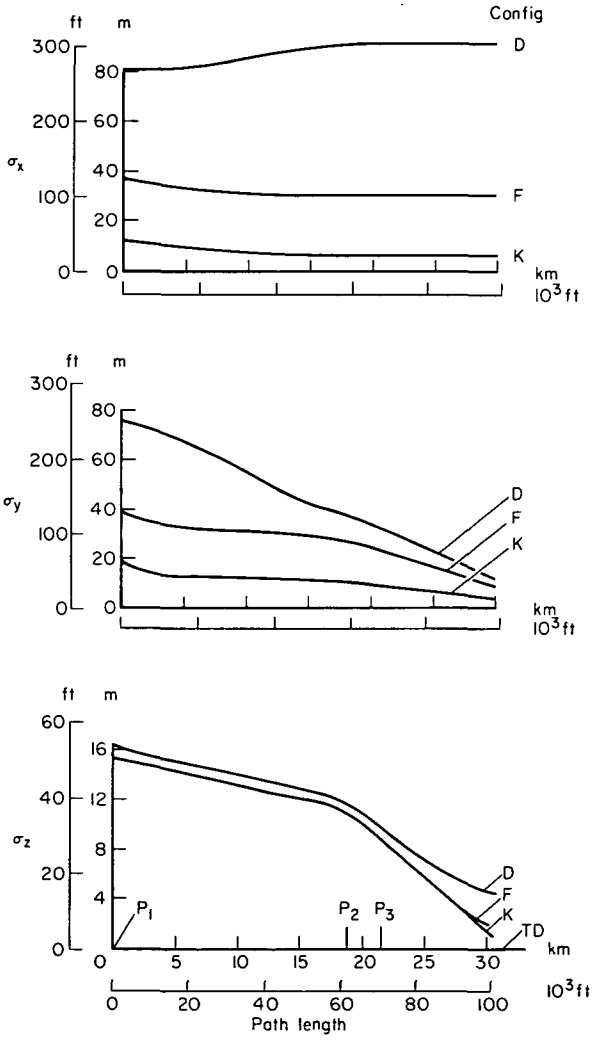

Figure 11(b).– Position estimation accuracy for example approach – bias limit.

For purposes of comparison, current arrival time errors at the outer market have an RMS error of around 30 sec, or 1.8 to 2.3 km (6000 to 7500 ft) in longitudinal position errors. A desired performance figure for future ATC is 5 sec (about 0.3 km). Insofar as estimation of position in the horizontal plane affects the arrival time performance, an accuracy of about 150 m RMS error has been judged adequate to meet the 5 sec performance figure. As seen in figures 9 and 11, the MLS configuration K exceeds by an order of magnitude this required position accuracy for the terminal area navigation region of the coverage.

RÉSUMÉ

The accuracy of determining position from the range, azimuth, and elevation data provided by microwave landing guidance system is investigated in this report. The RTCA SC–117 configurations D, F and K MLS models (ref. 1) are taken as the basis of the investigation as regards accuracy standards, coverage, and siting (tables 1 and 2). These accuracy standards are criteria expected to be met by the combined ground and airborne systems in providing values of the aircraft range, azimuth, and elevation. The principal variations in accuracy among these configurations are that range accuracy varies by a factor of 15, azimuth accuracy by a factor of 2, and elevation accuracy by a factor of 1.3. The DME error is almost entirely bias, while both bias and random errors of significant size occur in the angle errors. Both types of errors are included in the calculations.

Formulas for determining the Cartesian coordinates of the aircraft position relative to the runway from the MLS variables are given (eqs. (1) to (6)). These equations are appropriate for inverting current values of range, azimuth, and elevation, as in the case of inverting the outputs of a sample-and-hold system (e.g., ref. 6). The covariance of position determination errors is given in terms of the MLS accuracy (eqs. (8) to (10)) along with individual formulas for the RMS errors (eq. (11)), and these equations are used for the computational results of this report.

These formulas and the results apply to the simpler uses of the MLS data in which single samples of each of the three data types are inverted directly to produce position coordinates or glide-slope deviation. Digital data processing schemes, in which the path estimate is fitted to a span of recent data, are required for estimating velocity from the MLS data. In such cases the position determination accuracy is limited by the system bias errors, and this limit does not permit significant improvement over the results given here from both random and bias errors. Connsequently, insofar as position determination is concerned, the present results reflect reasonably well the accuracy obtainable from any treatment of the MLS data.

For purposes of discussion, the MLS coverage is divided into a flare region, final approach region, and terminal area navigation region, corresponding to a division of terminal area landing operations into flare and touchdown, glide-slope intercept and tracking, and terminal area approach to the glide slope.

For the flare region, interest is limited to configuration K, which provides a flare antenna for use in implementing category III automatic flare and landing. The flare maneuver is initiated at 9 to 15 m (30 to 50 ft) altitude, and touchdown occurs somewhere in the first 1000 m of runway. The results for RMS position determination errors in this region are

$$\sigma_x = \sigma_d = 20 \text{ ft} = 6.1 \text{ m}$$

$$\sigma_y = L_A \, \sigma_{AZ} = 9 \text{ to } 10 \text{ ft} \cong 3 \text{ m}$$

$$\sigma_z = L_E \, \sigma_{EL} = 1 \text{ to } 3 \text{ ft} = 0.3 \text{ to } 0.9 \text{ m}$$

Deterioration of the DME accuracy affects the x-accuracy directly, and to a minor degree, the altitude accuracy. Altitude determination accuracy during flare is comparable to the category II radar altimeter standard and to the accuracies achieved by current radar altimeters. Altitude rate performance is also important in assessing the suitability of the EL_2–DME combination as the source of flare region altitude data, but figures for this parameter are beyond the present scope.

The location of the flare antenna is bracketed by decreasing accuracy with incrreasing distance from the touchdown point and by the necessary touchdown point dispersion allowance.

In the final approach region, that is, in the center plane from the runway threshold out to about 15 km, typical flight paths for which position data are to be provided by the MLS are straight-in approaches, with glide-slope interception at about 5 n. mi. (9 km), and standard glide slopes of 2.5° to 3.0° down to the decision height altitude 30 to 60 m (100 to 200 ft) or alert height. The MLS can also supply navigation data for potential flight operations such as two-segment noise abatement approaches or any path contained within its coverage. Flight altitudes are usually below 1 km in this region. Results for this region are generally approximated by

$$\sigma_x \cong \sigma_d$$

$$\sigma_y = L_A \, \sigma_{AZ}$$

$$\sigma_z = \sqrt{L_E^2 \, \sigma_{EL}^2 + \tan^2 EL \, \sigma_d^2} \cong L_E \, \sigma_{EL}$$

The first formula for altitude error includes the DME error contribution, which is significant at close distances, and poorer DME accuracy standards. The RMS errors at several points of interest on the final approach flight path are given in table 4.

Accuracy for the linear glide-slope deviation ($\Delta z = -L_E \Delta EL_1$) is given by

$$\sigma_{\Delta z} \cong L_E \, \sigma_{EL}$$

so that performance in determining this variable is the same as for altitude, except near the decision height. Performance figures at the decision height are given in table 4. The difference is due to the first-order effect of the DME error on altitude accuracy at distances close to the elevation antenna.

TABLE 4.– RSM POSITION DETERMINATION ERRORS ON THE FINAL APPROACH, IN FEET

SC-117 config.	K		F		D	
	ft	m	ft	m	ft	m
σ_x	20	6.1	100	30	300	91
σ_y Threshold	10	3	20	6.1	17	5.2
Outermarker	32	9.8	70	21.4	91	28
15 km	47	14.3	102	31.2	138	42
σ_z Decision height	2–4	0.6–1.2	5–7	1.5–2.1	14–17	4.3–5.2
Outermarker	30	9.1	30	9.1	40	12.2
15 km	53	16.2	53	16.2	68	16.2
$\sigma_{\Delta z}$ Decision height	2–4	0.6–1.2	2–4	0.6–1.2	5–6	1.5–1.8

is due to the first-order effect of the DME error on altitude accuracy at distances close to the elevation antenna.

Finally, accuracy throughout the remainder of the MLS coverage is explored. The MLS, configuration K, is expected to provide the high precision path information basic to future high density air traffic control within 40 km or more from the runway. Results are given for two terminal area flight paths. Performance is 12 to 18 m (40 to 60 ft) RMS error or better in all three coordinates for both trajectories. Both y and z accuracy improve with decreasing distance to touchdown while x accuracy reaches a limit set by the DME bias as the aircraft approaches the center plane. Generally, RMS errors in this region are approximated by

$$\sigma_x \cong \sqrt{\cos^2 AZ\ \sigma_d^2 + y^2\ \sigma_{AZ}^2}$$

$$\sigma_y \cong \sqrt{\sin^2 AZ\ \sigma_d^2 + L_A^2\ \sigma_{AZ}^2}$$

$$\sigma_z \cong L_E\ \sigma_{EL}$$

that is, performance for the horizontal plane coordinates depends on the DME and azimuth accuracy, and altitude performance depends on elevation accuracy. Results are also given for configurations F and D, for which performance degrades principally in the horizontal plane coordinates as a result of the poorer DME and azimuth accuracies. These results do not reflect possible off-course deterioration in system accuracy, for lack of a suitable model. The permitted deterioration is limited to a factor of 2 (ref. 1).

The configuration K performance in determining position is excellent when compared to the position determination accuracy required to achieve air traffic control performance of 5 sec RMS error in arrival at the glide-slope intercept.

The estimation of range rate from range data was also discussed in this paper. The SC-117 standards require that the random component of the range error be such that a range rate accuracy of 3.05 m/sec (10 ft/sec) be achieved by averaging range samples over 0.2 sec. It was determined that the required RMS random range error is 0.6 m (2 ft).

A subject for further research is the estimation of velocity from the position data provided by the MLS. A method of estimating velocity was investigated for the one-dimensional example of range-rate estimation. This method consists of a least-squares fit of the estimated position time history to data obtained from the MLS during a limited averaging interval. The obtainable velocity accuracy will be a function of the length of the averaging interval, the MLS data rate, the MLS accuracy standards, and the bounds on aircraft acceleration within the MLS coverage. Of these factors, the last three are likely to be fixed and a corresponding optimum averaging interval can be determined, as well as the variation of the optimum accuracy with MLS data rates. A related problem area is that of providing an efficient data processing algorithm with which the averaging interval can be selected independent of the rate at which the velocity estimate is updated.

Ames Research Center
National Aeronautics and Space Administration
Moffett Field, California 94035, July 18, 1972

APPENDIX A

DERIVATION OF ERROR FORMULAS

The aircraft position in the runway coordinate frame (x,y,z) and in the variables of the LGS (d, AZ, EL) are related by equations (1) and (3) of the text. These are repeated here for convenience:

$$\left.\begin{aligned} L_A \tan AZ - y &= 0 \\ L_E \tan EL + z &= 0 \\ L_A{}^2 + y^2 + z^2 - d^2 &= 0 \end{aligned}\right\} \tag{A1}$$

The relation between errors or small deviations of x,y,z and the variables of the MLS is given by

$$\begin{pmatrix} \tilde{x} \\ \tilde{y} \\ \tilde{z} \end{pmatrix} = H_r \begin{pmatrix} \tilde{d} \\ \tilde{AZ} \\ \tilde{EL} \end{pmatrix} \tag{A2}$$

where

$$H_r = \begin{bmatrix} \partial x/\partial d & \partial x/\partial AZ & \partial x/\partial EL \\ \partial y/\partial d & \partial y/\partial AZ & \partial y/\partial EL \\ \partial z/\partial d & \partial z/\partial AZ & \partial z/\partial EL \end{bmatrix}$$

The required partial derivatives can be found by taking partials of equation (A1) with respect to d, AZ, EL hence

$$\left.\begin{aligned} \frac{\partial x}{\partial d} \tan AZ + \frac{\partial y}{\partial d} &= 0 \\ -\frac{\partial x}{\partial d} \tan EL + \frac{\partial z}{\partial d} &= 0 \\ -L_A \frac{\partial x}{\partial d} + y \frac{\partial y}{\partial d} + z \frac{\partial z}{\partial d} - d &= 0 \end{aligned}\right\} \tag{A3}$$

$$\left.\begin{aligned} \frac{L_A}{\cos^2 AZ} - \frac{\partial x}{\partial AZ}\tan AZ - \frac{\partial y}{\partial AZ} &= 0 \\ -\frac{\partial x}{\partial AZ}\tan EL + \frac{\partial z}{\partial AZ} &= 0 \\ -L_A\frac{\partial x}{\partial AZ} + y\frac{\partial y}{\partial AZ} + z\frac{\partial z}{\partial AZ} &= 0 \end{aligned}\right\} \tag{A4}$$

$$\left.\begin{aligned} \frac{\partial x}{\partial EL}\tan AZ + \frac{\partial y}{\partial EL} &= 0 \\ \frac{L_E}{\cos^2 EL} - \frac{\partial x}{\partial EL}\tan EL + \frac{\partial z}{\partial EL} &= 0 \\ -L_A\frac{\partial x}{\partial EL} + y\frac{\partial y}{\partial EL} + z\frac{\partial z}{\partial EL} &= 0 \end{aligned}\right\} \tag{A5}$$

Equations (A3), (A4), and (A5) can be solved, respectively, for the partials with respect to d, AZ, and EL:

$$\begin{aligned} \frac{\partial x}{\partial d} &= \frac{d}{(z\tan EL - y\tan AZ - L_A)} \\ \frac{\partial x}{\partial AZ} &= \frac{-yL_A}{\cos^2 AZ\,(z\tan EL - y\tan AZ - L_A)} \\ \frac{\partial x}{\partial EL} &= \frac{zL_E}{\cos^2 EL\,(z\tan EL - y\tan AZ - L_A)} \end{aligned} \tag{A6}$$

The remaining partials are readily given in terms of these, using equations (A3) and (A5).

The final form of these expressions is a matter of choice; in the present case, define

$$\tan\psi \equiv -\frac{z}{L_A} \tag{A7}$$

which is the aircraft elevation as seen from the azimuth antenna site. The denominator in equation (A6) then becomes:

$$z\tan EL - y\tan AZ - L_A = -\frac{L_A}{\cos^2 AZ}(1 + \tan\psi\tan EL\cos^2 AZ) \tag{A8}$$

and also

$$\frac{d\cos^2 AZ}{L_A} = \cos AZ\sqrt{(L_A{}^2 + y^2 + z^2)\frac{\cos^2 AZ}{L_A{}^2}} = \cos AZ\sqrt{1 + \tan^2\psi\cos^2 AZ} \qquad \text{(A9)}$$

Finally, utilizing (A7) to (A9) in (A6), obtain the forms given in the text:

$$\left.\begin{aligned}
\frac{\partial x}{\partial d} &= -\cos AZ\,\frac{\sqrt{1 + \tan^2\psi\cos^2 AZ}}{1 + \tan\psi\tan EL\cos^2 AZ} \\
\frac{\partial x}{\partial AZ} &= \frac{y}{(1 + \tan\psi\tan EL\cos^2 AZ)} \\
\frac{\partial x}{\partial EL} &= \frac{L_E\tan\psi\cos^2 AZ}{\cos^2 EL\,(1 + \tan\psi\tan EL\cos^2 AZ)}
\end{aligned}\right\} \qquad \text{(A10)}$$

REFERENCES

1. Anon.: A New Guidance System for Approach and Landing. vol. 2, p. III (SC-117 Committee Reports) Radio Technical Commission for Aeronautics, 1717 H Street, N.W., Washington, D.C. Document DO-148, 18 Dec. 1970.

2. National Plan for the Development of the Microwave Landing System DOT/FAA, NASA, DOD. July 1971. AD733268.

3. Anon.: Criteria for Approval of Category II Landing Weather Minima. FAA Advisory Circular AC 120-20, Rules Service Co., Washington, D.C. 6 June 1966.

4. Anon.: Low Altitude Instrument Approach Procedures West U.S. DOD Flight Information Publication. Aeronautical Chart and Information Center, USAF, St. Louis, Missouri, vol. 2, Effective 4 Feb 1971–4 Mar 1971.

5. FAA Advisory Circular AC 120-28A. Criteria For Approval of Category IIIa Landing Weather Minima. DOT, FAA, Washington, D.C. 14 Dec 1971.

6. Cherry, George W.; MacKinnon, Duncan; DeWolf, Barton: Increasing Airport Capacity and Terminal Area Safety by Means of the SBILS. Instrum. Aerosp. Ind. Proc. ISA, vol. 16, May 1970, Seattle.

7. Neuman, Frank; and Foster, John D.: Investigation of a Digital Automatic Aircraft Landing System in Turbulence; NASA TN D-6066, 1970.

NASA-Langley, 1973 — 21 A-4176

NATIONAL AERONAUTICS AND SPACE ADMINISTRATION
WASHINGTON, D.C. 20546

OFFICIAL BUSINESS
PENALTY FOR PRIVATE USE $300

SPECIAL FOURTH-CLASS RATE BOOK

POSTAGE AND FEES PAID
NATIONAL AERONAUTICS AND SPACE ADMINISTRATION
451

U.S.MAIL

POSTMASTER: If Undeliverable (Section 158 Postal Manual) Do Not Return

"The aeronautical and space activities of the United States shall be conducted so as to contribute . . . to the expansion of human knowledge of phenomena in the atmosphere and space. The Administration shall provide for the widest practicable and appropriate dissemination of information concerning its activities and the results thereof."

—NATIONAL AERONAUTICS AND SPACE ACT OF 1958

NASA SCIENTIFIC AND TECHNICAL PUBLICATIONS

TECHNICAL REPORTS: Scientific and technical information considered important, complete, and a lasting contribution to existing knowledge.

TECHNICAL NOTES: Information less broad in scope but nevertheless of importance as a contribution to existing knowledge.

TECHNICAL MEMORANDUMS: Information receiving limited distribution because of preliminary data, security classification, or other reasons. Also includes conference proceedings with either limited or unlimited distribution.

CONTRACTOR REPORTS: Scientific and technical information generated under a NASA contract or grant and considered an important contribution to existing knowledge.

TECHNICAL TRANSLATIONS: Information published in a foreign language considered to merit NASA distribution in English.

SPECIAL PUBLICATIONS: Information derived from or of value to NASA activities. Publications include final reports of major projects, monographs, data compilations, handbooks, sourcebooks, and special bibliographies.

TECHNOLOGY UTILIZATION PUBLICATIONS: Information on technology used by NASA that may be of particular interest in commercial and other non-aerospace applications. Publications include Tech Briefs, Technology Utilization Reports and Technology Surveys.

Details on the availability of these publications may be obtained from:

SCIENTIFIC AND TECHNICAL INFORMATION OFFICE

NATIONAL AERONAUTICS AND SPACE ADMINISTRATION

Washington, D.C. 20546